Dissociation Dynamics

DOI: 10.1002/anie.201403859

State Selectivity and Dynamics in Dissociative Electron Attachment to CF_3I Revealed through Velocity Slice Imaging**

Frímann H. Ómarsson, Nigel J. Mason, E. Krishnakumar,* and Oddur Ingólfsson**

Abstract: *In light of its substantially more environmentally friendly nature, CF_3I is currently being considered as a replacement for the highly potent global-warming gas CF_4, which is used extensively in plasma processing. In this context, we have studied the electron-driven dissociation of CF_3I to form CF_3^- and I, and we compare this process to the corresponding photolysis channel. By using the velocity slice imaging (VSI) technique we can visualize the complete dynamics of this process and show that electron-driven dissociation proceeds from the same initial parent state as the corresponding photolysis process. However, in contrast to photolysis, which leads nearly exclusively to the $^2P_{1/2}$ excited state of iodine, electron-induced dissociation leads predominantly to the $^2P_{3/2}$ ground state. We believe that the changed spin state of the negative ion allows an adiabatic dissociation through a conical intersection, whereas this path is efficiently repressed by a required spin flip in the photolysis process.*

Trifluoroiodomethane, CF_3I, has an exceptionally short lifetime in the atmosphere of the earth (only a few days), and therefore its global-warming potential (GWP) is estimated to be less than 1.[1] Tetrafluoromethane, CF_4, on the other hand, is anticipated to have a lifetime of 50000 years in the atmosphere and a GWP of about 6000.[1] In the context of more environmentally friendly chemistry, CF_3I is thus currently being considered as a replacement gas for CF_4 in plasma processes used in the semiconductor industry. Furthermore, even though atomic iodine is considerably more effective than chlorine or bromine in the destruction of stratospheric ozone, CF_3I has an ozone-depletion potential that is only a fraction of that of the chlorinated or brominated analogues.[2]

The short lifetime of CF_3I in the atmosphere is primarily attributed to efficient photolytic cleavage of the CF_3–I bond through excitation to the A-band, which absorbs from about 350 to 200 nm.[3] This band is composed of three electronic excitations, which are represented in the Mulliken notation as $^3Q_1$, $^3Q_0$, and $^1Q_1$.[4] The $^3Q_0$ state results from a $\sigma\rightarrow\sigma^*$ transition, is of A_1 symmetry, and converges to the dissociation asymptote to yield iodine atoms in their excited $^2P_{1/2}$ state. The other two states both result from $n\rightarrow\sigma^*$ transitions, are of E symmetry, and converge to the dissociation asymptote to give iodine in its $^2P_{3/2}$ ground state. The potential-energy curves describing the dissociation of the CF_3–I bond from the $^3Q_0$ and $^1Q_1$ states are depicted semischematically with solid lines (as adapted from Ref. [5]) in Figure 1. In the Franck–Condon region, the $^1Q_1$ state is higher in energy than the $^3Q_0$ state, thus leading to a crossing of the potential-energy curves on the path along their respective dissociation asymptotes.

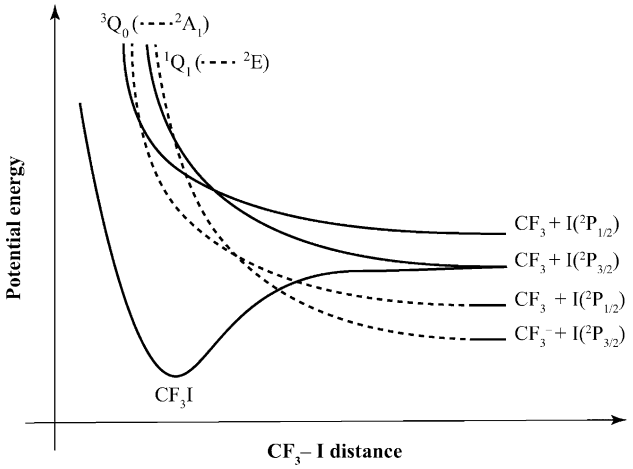

Figure 1. Schematic potential-energy curves for the neutral ground state of CF_3I and the $^3Q_0$ and $^1Q_1$ excited states (solid lines), and for the corresponding $^2A_1$ and ^2E core-excited negative-ion states (dotted lines). Curves for the neutral states are adapted from Ref. [5].

The photodissociation dynamics of CF_3I have been studied quite extensively.[3–5] The general picture has emerged that the oscillator strength of the A-band is mainly in the transition to the $^3Q_0$ state with A_1 symmetry, and that photodissociation of the CF_3–I bond proceeds primarily in a diabatic manner along the $^3Q_0$ potential surface, thus

[*] Dr. F. H. Ómarsson, Prof. Dr. O. Ingólfsson
Science Institute and Department of Chemistry
University of Iceland
Dunhagi 3, 107 Reykjavík (Iceland)
E-mail: odduring@hi.is
Prof. Dr. N. J. Mason
Department of Physical Sciences, The Open University
Walton Hall, MK7 6AA, Milton Keynes (UK)
E-mail: nigel.mason@open.ac.uk
Prof. Dr. E. Krishnakumar
Tata Institute of Fundamental Research
Homi Bhabha Road, Colaba, Mumbai 400005 (India)
E-mail: ekkumar@tifr.res.in

[**] F.H.Ó. acknowledges a grant from the Eimskip University Fund and a travel grant from the COST action CM0601 (ECCL). F.H.Ó. and O.I. acknowledge the Icelandic Center for Research (RANNÍS) for financial support. E.K. acknowledges a Marie Curie Fellowship.

Supporting information for this article is available on the WWW under http://dx.doi.org/10.1002/anie.201403859.

leading to the excited I atom ($^2P_{1/2}$). This process was already shown in 1987 by Gedanken,[6] who used magnetic circular dichroism to determine the contributions from the individual states. He reported that 84% of the oscillator strength of the A-band was due to the $^3Q_0$ state, which yielded the excited I atom ($^2P_{1/2}$), whereas 9 and 7% were due to the $^1Q_1$ and $^3Q_1$ states, respectively, which yielded the ground state I atom ($^2P_{3/2}$). These ratios are important when considering CF_3I as a plasma-processing gas, as the energy difference between these two states of iodine is 0.94 eV.[7] This difference will be reflected in the kinetic-energy release (KER) in the dissociation process and more importantly in the internal energy of the CF_3 fragment, which subsequently determines the reactive chemistry.

Despite the fact that plasma processes are largely electron-driven, electron-induced dissociation of CF_3I has received much less attention than the corresponding photolytic process. Christophorou and Olthoff[8] provided an authoritative review of electron interactions with CF_3I in 2000. The most comprehensive studies on dissociative electron attachment (DEA) to CF_3I were made by the Illenberger group in Berlin in the 1980s and 1990s.[9,10] In these studies, they showed that DEA to CF_3I proceeds through two resonances: a resonance close to 0 eV that exclusively yields I^- with high KER, and a core-excited resonance close to 3.8 eV that is associated with electronic excitation to the antibonding $\sigma^*_{CF_3-I}$ LUMO,[10] concomitant with electron capture. This resonance is thus expected to be associated with the $^2A_1$ or ^2E transient negative ion (TNI) states corresponding to the $\sigma\rightarrow\sigma^*$ and $n\rightarrow\sigma^*$ A-band transition in the neutral molecule, respectively. The TNI relaxes by dissociation (DEA) to form F^- and IF^- with low KER, thus suggesting a three-body breakup, and to form CF_3^- with exceptionally high KER through direct dissociation ascribed to a two-electron occupation of the $\sigma^*_{CF_3-I}$ LUMO. This process is analogous to the photodissociation observed through the A-band, as shown in Figure 1, in which the potential-energy curves of the $^2A_1$ and ^2E TNIs (dotted lines) and the corresponding $^3Q_0$ and $^1Q_1$ parent states (solid lines) are shown schematically. The dotted curves are purely schematic, except for the dissociation limits, which are lowered by the 1.82 eV electron affinity of CF_3[11] as compared to the corresponding neutral states. Furthermore, owing to the extra electron, we expect these TNIs to be destabilized at short and intermediate nuclear separation as compared to the neutral parent states.

Herein we present an experimental study on DEA to CF_3I on the basis of the velocity slice imaging (VSI) technique[12] to elucidate the state selectivity and the dynamics of this process in the energy range corresponding to the respective A-band. The VSI instrument is similar to that described by Nandi et al.,[13] except that the detector consists of three (80 mm) microchannel plates and a phosphor screen. An effusive gas beam is crossed with a magnetically collimated, pulsed electron beam with an energy resolution of about 0.5 eV. The electron attachment is confined to the overlap of the electron and molecular beams, but through the kinetic-energy release in the DEA process, the fragments extend in space to form a Newton sphere. After a 200 ns delay, the ions are extracted into a time-of-flight mass spectrometer, and a thin, center slice of the Newton sphere is recorded with the position sensitive detector by pulsing its voltage with an on-time of 100 ns. The center slice of the Newton sphere contains full information on the velocity and angular distributions of the anions formed. This allows us to deduce the symmetry of the transient negative ion state formed and, by calibrating with O^- formation in DEA to O_2 at 6.5 eV, we can derive the KER in the respective processes (see the Supporting Information and Refs. [14–16]).

Figure 2 shows a CF_3^- ion-yield curve recorded in the energy range from about 1.5 to 10 eV, and the left side of Figure 3 shows the velocity slice images (VSIs) recorded at

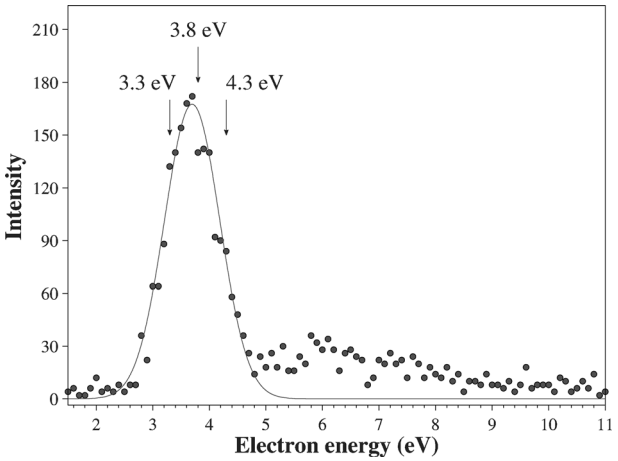

Figure 2. Ion-yield curve for CF_3^-. The arrows indicate at which points VSIs were taken. The solid line is only meant to guide the eye.

the energies indicated by the arrows in Figure 2, that is, at the rising edge, the center, and the falling edge of the CF_3^--ion yield. On the right side of Figure 3, the corresponding fits to the angular distributions are shown. As these angular distributions are symmetrical around the electron beam (white arrows in Figure 3), the fits are only shown for the range from 0 to 180°. From the VSIs, it is clear that the CF_3^- ion yield is composed of two discrete components: a low KER component appearing in the center of the figures, and a high KER component apparent as the outer circle. For a single bond rupture in DEA, the thermochemical threshold is given by the difference between the respective bond-dissociation energy (BDE) and the electron affinity (EA) of the charge-retaining fragment. In the current case, $E_{th} = BDE(CF_3-I) - EA(CF_3)$, and with $EA(CF_3) = 1.82$ eV[11] and $BDE(CF_3-I) = 2.35$ eV,[17] the threshold for CF_3^- formation is at 0.53 eV when the iodine is formed in its $^2P_{3/2}$ ground state, and at 1.47 eV when it is formed in the $^2P_{1/2}$ excited state. The total available excess energy in the system that can appear in KER and in the internal energy of the fragments is given by the difference between the incident electron energy and these threshold values. Table 1 compares the total available excess energy in the I ($^2P_{3/2}$) and I ($^2P_{1/2}$) channels with the measured KER at the intensity maxima of the outer distributions.

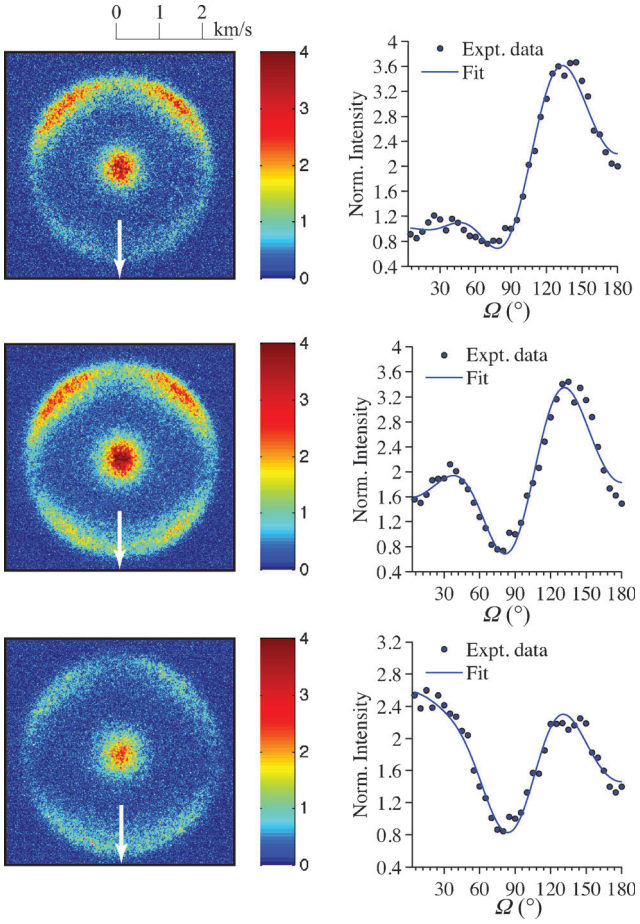

Figure 3. VSIs (left) and the respective fitted angular distributions (right) recorded at incident energies of 3.3 eV (top), 3.8 eV (middle), and 4.3 eV (bottom). Arrows in the VSIs indicate the direction of the electron beam. A normalized intensity scale is shown as a color map on the left side of the VSIs, and a velocity scale is shown at the top.

Table 1: Total available excess energy in the ground-state I ($^2P_{3/2}$) and first-excited-state I ($^2P_{1/2}$) channels as compared with the KER at the peak of its distribution. All values are in eV.

Electron energy	3.3	3.8	4.3
E_{excess} ($^2P_{3/2}$)	2.8	3.3	3.8
E_{excess} ($^2P_{1/2}$)	1.8	2.3	2.8
Measured KER	2.1	2.6	2.9

Figure 4 shows the respective KER distribution at an incident electron energy of 3.8 eV, with the total available excess energy in the I ($^2P_{3/2}$) and I ($^2P_{1/2}$) channels indicated with dashed vertical lines. Although the finite electron energy resolution causes some broadening (as evidenced by the tail above the I ($^2P_{3/2}$) threshold), it is clear from these comparisons that the bulk of the KER distribution is in all cases above the available excess energy for the excited state I ($^2P_{1/2}$) channel. Furthermore, the distribution observed is typical for a single DEA channel from a polyatomic molecule, that is, with a low-energy tail that reflects the population of excited vibrational modes of the fragment(s)[18] (CF_3^- in this case). From thermochemical considerations, this channel can only

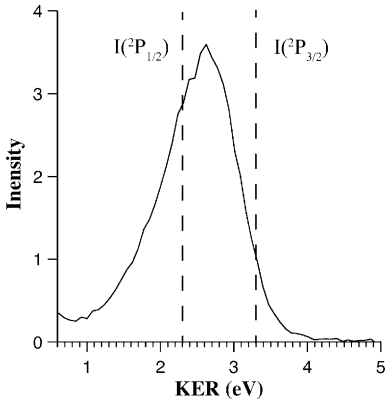

Figure 4. KER distribution at an incident electron energy of 3.8 eV. The total available excess energy in the I ($^2P_{3/2}$) and I ($^2P_{1/2}$) channels are indicated with dashed vertical lines.

be attributed to the formation of iodine in its ($^2P_{3/2}$) ground state. Also, the difference of about 0.94 eV between the threshold energies for I ($^2P_{3/2}$) and I ($^2P_{1/2}$) formation is too large not to be seen as a distinct discontinuity in the distribution if there were any significant contribution from the ($^2P_{1/2}$) channel. We thus attribute the outer, high-KER contribution to the formation of iodine in its $^2P_{3/2}$ ground state, although we cannot exclude a minor contribution from the $^2P_{1/2}$ channel. In contrast the low-KER component forming the isotropic distribution in the center of the VSIs may be due to dissociation into CF_3^- and excited I ($^2P_{1/2}$), with the remaining excess energy in internal excitation of the CF_3^- fragment. This contribution, however, might also be related to the three-body breakup leading to the formation of IF^-, that is, a slow process with effective internal-energy distribution, again leaving the bulk of the excess energy in the CF_3^- fragment.

The relative intensities of the two different dissociation channels can be estimated directly from the VSIs by integrating their measured intensity distribution over the whole Newton sphere. In the current experiment (100 ns detector on-time), the detected ion slice is about 1.6 mm thick, which is close to the diameter of the inner sphere of the low-KER ions. The diameter of the outer sphere, on the other hand, is about 24 mm. Thus, the bulk of the low-kinetic-energy fraction is detected directly, whereas only a fraction of the sphere containing the high-KER ions is recorded. By taking this into account and integrating the measured intensity distributions over the whole Newton sphere, we find that about 96–98% of the total ion signal is from the high-KER component. Within the accuracy of this approach, this percentage is independent of the incident electron energy, and despite some variation between the data sets, it is clear that at least 95% of the total ion signal is from the high-KER contribution. Hence, even if a small fraction of the high-KER contribution is from the excited-state ($^2P_{1/2}$) channel, the predominating relaxation channel leads to formation of iodine in its ($^2P_{3/2}$) ground state.

Turning back to the angular distribution shown in Figure 3, it is clear from visual inspection of the VSIs alone that there is a contribution in both the forward (180°) and

backward (0°) directions. A finite intensity in these directions can only result from an s-wave contribution, which again is only allowed for A_1 symmetry. None of the partial waves allowed in E symmetry can provide this angular distribution and we may thus conclude that this resonance must be associated with the A_1-symmetry $^3Q_0$ component of the A-band. This hypothesis was confirmed by fitting the angular distributions by using the basis functions for the irreducible representations of the C_{3v} point group. These fits are shown on the right side of Figure 3, with contributions from angular-momentum quantum numbers $l = 0$, 1, 2, and 3 and a difference of projection of the orbital angular momentum along the principal molecular axis of the resonant and target states, $\mu = 0$. For these values, which are those allowed for A_1, we obtain excellent agreement for the angular distributions (see the Supporting Information and Refs. [14–16] for further details).

We thus conclude that in DEA to CF_3I, the initial TNI state corresponds to a $^2A_1$ core-excited resonance associated with the same $\sigma \rightarrow \sigma^*$ excitation observed to carry the bulk of the oscillator strength in photodissociation. However, unlike the photodissociation process, this core-excited resonance relaxes predominantly in an adiabatic manner through the conical intersection between the $^2A_1$ and ^2E anionic states, which correspond to the $^3Q_0$ and $^1Q_1$ neutral states, as depicted in Figure 1.

The most plausible explanation for this fundamentally different dissociation dynamics in DEA as compared to photodissociation lies in the spin multiplicity of the involved states. Explicitly, whereas a transition from the $^3Q_0$ to the $^1Q_1$ neutral state requires a spin flip, no such spin flip is required for the corresponding $^2A_1$ and ^2E states. The relative shift of the potential-energy curves of the $^2A_1$ and ^2E states as compared to those of the $^3Q_0$ and $^1Q_1$ parent states may also favor this transition. This possibility is, however, speculative at this point and remains to be verified by high-level theory.

Received: March 31, 2014
Revised: August 6, 2014
Published online: September 15, 2014

Keywords: conical intersections · dissociative electron attachment · plasma chemistry · trifluoroiodomethane · velocity slice imaging

[1] A. K. Jain, B. P. Briegleb, K. Minschwaner, D. J. Wuebbles, *J. Geophys. Res. [Atmos.]* **2000**, *105*, 20773 – 20790.
[2] C. Clerbaux, D. M. Cunnhold, *Scientific Assessment of Ozone Depletion: 2006*, WMO (World Meterological Organization), Geneva, Switzerland, **2007**.
[3] N. J. Mason, P. Limão-Vieira, S. Eden, P. Kendall, S. Pathak, A. Dawes, J. Tennyson, P. Tegeder, M. Kitajima, M. Okamoto, *Int. J. Mass Spectrom.* **2003**, *223*, 647 – 660.
[4] R. S. Mulliken, *J. Chem. Phys.* **1940**, *8*, 382.
[5] V. N. Lokhman, D. D. Ogurok, E. A. Ryabov, *Eur. Phys. J. D* **2007**, *46*, 59 – 67.
[6] A. Gedanken, *Chem. Phys. Lett.* **1987**, *137*, 462 – 466.
[7] J. I. Steinfeld, R. N. Zare, L. Jones, M. Lesk, W. Klemperer, *J. Chem. Phys.* **1965**, *42*, 25 – 33.
[8] L. G. Christophorou, J. K. Olthoff, *J. Phys. Chem. Ref. Data* **2000**, *29*, 553 – 569.
[9] M. Heni, E. Illenberger, *Chem. Phys. Lett.* **1986**, *131*, 314 – 318.
[10] T. Oster, O. Ingólfsson, M. Meinke, T. Jaffke, E. Illenberger, *J. Chem. Phys.* **1993**, *99*, 5141.
[11] H.-J. Deyerl, L. S. Alconcel, R. E. Continetti, *J. Phys. Chem. A* **2001**, *105*, 552 – 557.
[12] F. H. Ómarsson, E. Szymańska, N. J. Mason, E. Krishnakumar, O. Ingólfsson, *Phys. Rev. Lett.* **2013**, *111*, 063201.
[13] D. Nandi, V. S. Prabhudesai, E. Krishnakumar, A. Chatterjee, *Rev. Sci. Instrum.* **2005**, *76*, 053107.
[14] T. F. O'Malley, H. S. Taylor, *Phys. Rev.* **1968**, *176*, 1 – 15.
[15] M. Tronc, C. Schermann, R. I. Hall, F. Fiquet-Fayard, *J. Phys. B* **1977**, *10*, 305 – 321.
[16] F. H. Ómarsson, O. Ingólfsson, N. J. Mason, E. Krishnakumar, *Eur. Phys. J. D* **2012**, *66*, 51.
[17] Y.-R. Luo, *Comprehensive Handbook of Chemical Bond Energies*, CRC, Boca Raton, FL, **2007**.
[18] N. B. Ram, V. S. Prabhudesai, E. Krishnakumar, *J. Phys. B* **2009**, *42*, 225203.

